Strong intermolecular interactions between selenium atoms of adjacent P_4Se_3 molecules are implied by the results of a recent redetermination of the X-ray structure of P_4Se_3. The selenium–selenium interactions produce helical chains of P_4Se_3 molecules directed along the unit cell *a* and *b* axes. There are four layers containing *a*- and *b*-directed helical chains per unit cell. This structure has certain similarities with the helical chain configuration found for trigonal selenium and may explain why P_4Se_3 decomposes slowly to form red amorphous selenium.

Acknowledgment. G.R.B. is grateful to the Council of Victoria University of Wellington for granting a sabbatical leave, held at University College London, during which much of this work was completed.

Registry No. P_4Se_3, 1314-86-9.

---

(23) Zallen, R.; Slade, M. L. *Phys. Rev. B: Solid State* **1974**, *B9*, 1627.

Contribution from the Department of Chemistry,
Louisiana State University, Baton Rouge, Louisiana 70803-1804

X-ray Single-Crystal Structure Determination of Copper(II), Cobalt(II), and Nickel(II) Complexes of 2,2-Bis(2-pyridyl)- and 2,2-Bis(6-methyl-2-pyridyl)-1,3-dioxolane[1]

George R. Newkome,* Hellen C. R. Taylor, Frank R. Fronczek, and Vinod K. Gupta

Received June 26, 1985

2,2-Bis(2-pyridyl)- and 2,2-bis(6-methyl-2-pyridyl)-1,3-dioxolane readily formed chelates with Co(II), Ni(II), and Cu(II). X-ray analysis of the Cu(II) and Co(II) complexes showed primary N-chelation through the pyridines with a moderate interaction to one of the dioxolane oxygens. In the octahedral Ni(II) complex of the methylpyridyl ketal, the ligand was bound to the metal in a tridentate fashion. $CuCl_2C_{13}H_{12}N_2O_2$ (**4**) is monoclinic, $P2_1/c$, $a = 9.022$ (2) Å, $b = 12.053$ (3) Å, $c = 13.564$ (5) Å, $\beta = 108.50$ (3)°, $Z = 4$, and $R = 0.029$ for 3107 observations. $CuCl_2C_{15}H_{16}N_2O_2$ (**5**) is triclinic, $P\bar{1}$, $a = 8.221$ (3) Å, $b = 9.265$ (4) Å, $c = 11.351$ (3) Å, $\alpha = 99.89$ (3)°, $\beta = 100.21$ (3)°, $\gamma = 100.08$ (3)°, $Z = 2$, and $R = 0.035$ for 2267 observations. $CoCl_2C_{15}H_{16}N_2O_2$ (**7**) is monoclinic, $P2_1/n$, $a = 8.658$ (1) Å, $b = 11.127$ (4) Å, $c = 16.731$ (4) Å, $\beta = 90.28$ (2)°, $Z = 4$, and $R = 0.036$ for 2233 observations. $[Ni(C_{15}H_{16}N_2O_2)(H_2O)_3]Cl_2$ (**10**) is orthorhombic, *Pbca*, $a = 12.185$ (4) Å, $b = 13.820$ (5) Å, $c = 21.881$ (4) Å, $Z = 8$, and R = 0.033 for 2423 observations.

Introduction

Bidentate bis(2-pyridyl) ketone (**1**) can exhibit two modes of coordination: N,O-coordination generating a five-membered chelate ring and N,N-coordination (six-membered chelate), which are easily differentiated by the magnitude of the carbonyl stretching frequency [ν(CO)] in the IR spectrum.[2] In the free ligand, the electron-poor nature of the pyridines reduces the carbonyl bond order, as evidenced by the comparatively low ν(CO) in **1b**: 1675 cm^{-1}.[3] O-Coordination should further diminish ν(CO), whereas N,N-coordination should increase the carbonyl bond order relative to **1**, and a shift ν(CO) to higher frequencies should be observed.

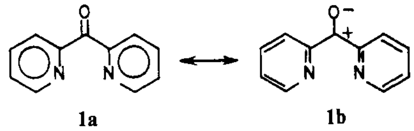
1a **1b**

Osborne and McWhinnie reported[2] the first preparation of Cu(II) complexes of **1** and attributed changes in ν(CO) to an alteration in the mode of complexation from N,O to N,N. Several transition-metal [Mn(II), Fe(II), Co(II), Cu(II), and Ni(II)] complexes with **1** have been prepared and were proposed to be N,N-chelated on the basis of numerous similarities observed in the IR spectra of $[M(\mathbf{1})X_2]$.[3] It has been also reported[2] that water adds across the ketone of N,N-coordinated **1** to affored stable *gem*-diols. Further studies[4,5] have demonstrated that nucleophiles add after the formation of the N,N-coordinated complex and that the serendipitous disposition of X provides the possibility of tridentate chelation by carbonyl adducts of **1**[6] (Figure 1).

More recent examples of **1** with U(IV),[7] Zn(II), Cd(II), and Hg(II),[8] and lanthanides [as Ln(III)][9] have been reported. In its hydrated form, **1** forms a (μ-peroxo)dicobalt(III) complex,[10] $[Co_2(\mathbf{1}\cdot H_2O)_4(py)_2O_2](ClO_4)_4$, upon oxygenation of the corresponding Co(II) complex. The Pd(II), Pt(II), and Au(III) chlorides also react with **1** to give complexes in which one or two ligand molecules, either the carbonyl or the *gem*-diol form, are coordinated to the metal ion.[11]

Numerous transition-metal complexes of **1** display a proclivity for nucleophilic addition to a carbonyl group as well as the stability of the "hydrate" complexes that result. Since both 2,2-bis(2-pyridyl)-1,3-dioxolane (**2**) and 2,2-bis(6-methyl-2-pyridyl)-1,3-dioxolane (**3**) possess a spiroketal function that can mimic the "hydrated" form of **1**, we investigated the complexation properties of these ligands with Co(II), Ni(II), and Cu(II). In our earlier work we reported a novel series of (malonate ester-*C*)palladium complexes of **2** and conducted structural analysis to provide a

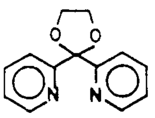
2

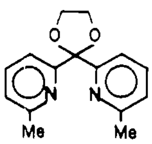
3

---

(1) Chemistry of Heterocyclic Compounds. 117. Part 116: Fronczek, F. R.; Taylor, H. C. R.; Gupta, V. K.; Newkome, G. R. *Acta Crystallogr., Sect. C: Cryst. Struct. Commun.* **1985**, *C41*, 1548.

(2) Osborne, R. R.; McWhinnie, W. R. *J. Chem. Soc. A* **1967**, 2075.

(3) Feller, M. C.; Robson, R. *Aust. J. Chem.* **1968**, *21*, 2919.

(4) Feller, M. C.; Robson, R. *Aust. J. Chem.* **1970**, *23*, 1997.

(5) Bakker, I. J.; Feller, M. C.; Robson, R. *J. Inorg. Nucl. Chem.* **1971**, *33*, 747.

(6) Fischer, B. E.; Sigel, H. *J. Inorg. Nucl. Chem.* **1975**, *37*, 2127.

(7) Ortego, J. D.; Perry, D. L. *J. Inorg. Nucl. Chem.* **1973**, *35*, 3031 and references cited therein.

(8) Ortego, J. D.; Upalawanna, S.; Amanoilahi, S. *J. Inorg. Nucl. Chem.* **1979**, *41*, 593.

(9) Jagannathan, R.; Soundarajan, S. *J. Inorg. Nucl. Chem.* **1980**, *42*, 145.

(10) Ortego, J. D.; Seymour, M. *Polyhedron* **1982**, *1*, 21.

(11) Annibale, G.; Canovese, L.; Cattalini, L.; Natile, G.; Biagini-Cingi, M.; Manotti-Lanfredi, A. M.; Tiripicchio, A. *J. Chem. Soc., Dalton Trans.* **1981**, *2280*.

(12) Newkome, G. R.; Gupta, V. K.; Theriot, K. J.; Ewing, J. C.; Wicelinski, S. P.; Huie, W. R.; Fronczek, F. R.; Watkins, S. F. *Acta Crystallogr., Sect. C: Cryst. Struct. Commun.* **1984**, *C40*, 1352.

(13) Newkome, G. R.; Gupta, V. K.; Taylor, H. C. R.; Fronczek, F. R. *Organometallics* **1984**, *3*, 1549.

0020-1669/86/1325-1149$01.50/0

Table I. Analytical Data and Description of Transition-Metal Complexes

complex	ligand	metal salt	weight,[a] mg	elemental anal., %[b] C	H	N	description[c]
4	**2**	$CuCl_2$	39.4	43.04 (43.14)	3.31 (3.23)	7.73 (7.75)	massive emerald green crystals[d]
6	**2**	$CoCl_2 \cdot 6H_2O$	69.7	33.48 (33.41)	2.58 (2.69)	6.01 (6.07)	massive magenta crystals
8	**2**	$NiCl_2 \cdot 6H_2O$	69.6	33.50 (33.37)	2.58 (2.65)	6.01 (6.03)	brilliant yellow powder
11	**2**	$PdCl_2$	53.2	38.49 (38.40)	2.96 (3.09)	6.91 (6.84)	yellow needles[e]
5	**3**	$CuCl_2$	39.4	46.10 (46.18)	4.10 (4.07)	7.17 (7.30)	massive dark green crystals[d]
7	**3**	$CoCl_2 \cdot 6H_2O$	69.7	36.44 (36.39)	3.24 (3.25)	5.67 (5.61)	dark blue prisms[d]
9	**3**	$NiCl_2 \cdot 6H_2O$	69.6	36.46 (36.54)	3.24 (3.22)	5.67 (5.70)	brilliant yellow powder[e]
10	**3**	$NiCl_2 \cdot 6H_2O$	69.6	48.84 (48.94)	5.97 (5.92)	7.59 (7.66)	massive light green crystals[d]
12	**3**	$PdCl_2$	53.2	41.54 (41.60)	3.69 (3.60)	6.46 (6.52)	yellow powder[e]

[a] 0.30 mmol. [b] Found (calcd). [c] All melting points >250 °C. [d] X-ray structure. [e] ^1H NMR in Table IX.

Table II. Crystal Data and Data Collection Parameters

	4	**5**	**7**	**10**
formula	$CuCl_2C_{13}H_{12}N_2O_2$	$CuCl_2C_{15}H_{16}N_2O_2$	$CoCl_2C_{15}H_{16}N_2O_2$	$[Ni(C_{15}C_{16}N_2O_2)(H_2O)_3]Cl_2$
M_r	362.7	390.8	386.2	440.0
cryst syst	monoclinic	triclinic	monoclinic	orthorhombic
space group	$P2_1/c$	$P\bar{1}$	$P2_1/n$	*Pbca*
a, Å	9.022 (2)	8.221 (3)	8.658 (1)	12.185 (4)
b, Å	12.053 (3)	9.265 (4)	11.127 (4)	13.820 (5)
c, Å	13.564 (5)	11.351 (3)	16.731 (4)	21.881 (4)
α, deg		99.89 (3)		
β, deg	108.50 (3)	100.21 (3)	90.28 (2)	
γ, deg		100.08 (3)		
V Å^3	1399 (1)	819 (1)	1612 (1)	3685 (3)
Z	4	2	4	8
D_c, g cm^{-3}	1.722	1.584	1.591	1.586
μ(Mo Kα), cm^{-1}	19.50	16.71	14.03	13.76
cryst size, mm	0.36 × 0.48 × 0.56	0.32 × 0.50 × 0.56	0.36 × 0.40 × 0.64	0.52 × 0.60 × 0.68
color	green	dark green	dark blue	light green
T, °C	27	26	25	27
2θ limits, deg	$2 \le 2\theta \le 60$	$2 \le 2\theta \le 50$	$2 \le 2\theta \le 50$	$2 \le 2\theta \le 50$
data collcd	$h,k,\pm l$	$h,\pm k,\pm l$	$h,k,\pm l$	h,k,l
scan speeds, deg min^{-1}	0.42–20.0	0.56–20.0	0.31–20.0	0.37–20.0
min rel trans coeff, %	85.68	79.63	98.60	86.19
R_{int}	0.018		0.023	
no. of unique data	4065	2870	2836	3234
no. of obsd data	3107	2267	2233	2423
no. of refined variables	230	200	200	315
extinction coeff	5.0 (5) × 10^{-7}	4.7 (16) × 10^{-7}	2.4 (8) × 10^{-7}	1.9 (3) × 10^{-7}
R	0.029	0.035	0.036	0.033
R_w	0.045	0.051	0.050	0.055
residual density, e Å^{-3}	0.67	0.44	0.26	0.41
H atom treatment	refined	located, ΔF	located, ΔF	refined

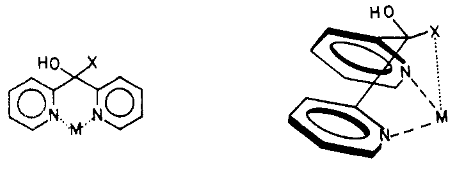

Figure 1.

model for a carbanion-ligand-exchange pathway. This study has been undertaken to determine the salient structural features of Co(II), Ni(II), and Cu(II) complexes of **2** and **3** and to ascertain the effect of the core metal in the microenvironment of these ligands, which will be subsequently helpful in studying the chloride–malonate ligand-exchange reactions on these complexes. Crystal structure analysis of the Pd(II) complexes of **2** exhibited a M···O contact, which suggested the possibility of **2** or **3** behaving as a tridentate ligand.[12] Such coordination was sought in complexes of first-row transition metals and found for the Ni(II) complex herein reported.

Results and Discussion

Brilliantly colored complexes were formed from **2** and **3** upon treatment with the chlorides of Cu(II), Co(II), and Ni(II) in anhydrous MeOH and with that of Pd(II) in CH_3CN.[12,13] All of the adducts melted or decomposed above 250 °C and displayed elemental analysis data that supported a 1:1 ligand-to-metal stoichiometry (Table I).

In order to determine the salient features, such as the modes of coordination of **2** and **3** and nature of M···O interactions, single crystals of complexes **4–12** were grown from various solvents; only **4**, **5**, **7**, and **10**, however, gave suitable crystals. The crystal data and data collection parameters are presented in Table II. Selected bond lengths, bond angles, and intermolecular contacts are given in Tables III and VII. Coordinates of non-hydrogen atoms for **4**, **5**, **7**, and **10** are presented in Tables IV, V, VI, and VIII, respectively.

Dichloro[2,2-bis(2-pyridyl)-1,3-dioxolane]copper(II) (4). Crystals of **4** consist of neutral molecules in which the Cu(II) is bound in a slightly distorted square-planar array of the two nitrogens and two chlorides (Figure 2a).

The pyridines are planar and form a dihedral angle of 70.5°; the flexibility of the ligand permits chelation to occur with a "bite" angle of 85.04 (5)°, very near the ideal value. The six-membered chelate ring, Cu–N1–C5–C6–C7–N2, adopts a boat conformation that leaves the Cu and C6 on the same side of the plane formed by the other four atoms.[11] The dioxolane ring, C6–O1–C12–C13–O2, exists as a half-chair in which C13 lies on the local pseudodiad axis; all of the atoms are twisted to the *same* side of the ligand as the metal. In fact, dioxolane O1 occupies a position near an axial site on the copper, which gives the complex an almost square-pyramidal appearance.[2] The Cu–O1 intramolecular interaction is weak, as indicated by the Cu–O1 distance [2.678 (1) Å]. The Cu–O1 vector tilts slightly away from the plane normal (toward the heteroaromatic rings), and the Cl1–Cu–Cl2 angle

Table III. Selected Bond Lengths (Å), Bond Angles (deg), and Contact Distances (Å) in Complexes **4**, **5**, **7**, and **11**

	4	**5**	**7**	**11**[a]
M–N1	2.024 (1)	2.136 (2)	2.062 (2)	2.035 (4)
M–N2	2.055 (1)	2.014 (2)	2.020 (2)	2.031 (4)
M–Cl1	2.269 (1)	2.204 (1)	2.271 (1)	2.288 (1)
M–Cl2	2.273 (1)	2.250 (1)	2.214 (1)	2.292 (1)
M–Cl2′	2.844 (1)			
M–O1	2.678 (1)	2.400 (2)	2.853 (2)	2.935 (3)
N1–M–N2	85.04 (5)	81.94 (7)	99.65 (6)	89.0 (1)
N1–M–Cl1	89.34 (4)	94.57 (6)	102.16 (5)	178.1 (3)
N1–M–Cl2	172.03 (4)	167.24 (6)	114.91 (5)	91.0 (1)
Cl1–M–Cl2	95.71 (2)	94.43 (3)	113.82 (3)	90.95 (5)
N2–M–Cl1	162.60 (4)	172.59 (5)	102.80 (5)	91.1 (1)
N2–M–Cl2	91.82 (4)	90.10 (6)	120.89 (5)	177.9 (5)
Cl1–M–Cl2′	104.17 (2)			
Cl2–M–Cl2′	83.32 (1)			
Cl2′–M–N1	89.47 (4)			
Cl2′–M–N2	92.25 (4)			

[a] Since the asymmetric unit contained two molecules, average bond distances and angles are reported here.[12]

Table IV. Coordinates of Non-Hydrogen Atoms for $CuCl_2C_{13}H_{12}N_2O_2$ (**4**)[a]

atom	*x*	*y*	*z*
Cu	0.03933 (2)	0.35604 (2)	0.45285 (2)
Cl1	−0.19854 (6)	0.29990 (5)	0.34796 (4)
Cl2	0.02681 (5)	0.52856 (4)	0.38304 (3)
O1	0.1829 (1)	0.2033 (1)	0.3720 (1)
O2	0.3765 (2)	0.0905 (1)	0.4666 (1)
N1	0.0584 (2)	0.2132 (1)	0.5344 (1)
N2	0.2764 (2)	0.3693 (1)	0.5242 (1)
C1	−0.0391 (2)	0.1895 (2)	0.5889 (2)
C2	−0.0268 (2)	0.0933 (2)	0.6455 (2)
C3	0.0854 (3)	0.0166 (2)	0.6439 (2)
C4	0.1865 (2)	0.0398 (2)	0.5883 (1)
C5	0.1687 (2)	0.1390 (1)	0.5344 (1)
C6	0.2757 (2)	0.1758 (2)	0.4746 (1)
C7	0.3651 (2)	0.2781 (2)	0.5285 (1)
C8	0.5241 (2)	0.2769 (2)	0.5827 (2)
C9	0.5929 (2)	0.3710 (2)	0.6332 (2)
C10	0.5022 (2)	0.4644 (2)	0.6295 (2)
C11	0.3452 (2)	0.4608 (2)	0.5741 (1)
C12	0.2827 (2)	0.1882 (2)	0.3098 (2)
C13	0.3972 (3)	0.1006 (3)	0.3668 (2)

[a] Estimated standard deviations in the least significant digits are shown in parentheses.

Table V. Coordinates of Non-Hydrogen Atoms for $CuCl_2C_{15}H_{16}N_2O_2$ (**5**)[a]

atom	*x*	*y*	*z*
Cu	0.80554 (4)	0.07902 (3)	0.77158 (3)
Cl1	0.58833 (9)	−0.02858 (8)	0.83787 (7)
Cl2	0.84506 (14)	−0.13772 (9)	0.66861 (10)
O1	0.6923 (2)	0.1575 (2)	0.5890 (2)
O2	0.7772 (3)	0.3741 (2)	0.5300 (2)
N1	0.7749 (3)	0.3019 (2)	0.8331 (2)
N2	1.0169 (3)	0.1903 (2)	0.7338 (2)
C1	0.7770 (5)	0.2888 (4)	1.0462 (3)
C2	0.7553 (4)	0.3681 (3)	0.9433 (3)
C3	0.7179 (5)	0.5109 (4)	0.9594 (3)
C4	0.7070 (5)	0.5866 (4)	0.8669 (4)
C5	0.7331 (4)	0.5198 (3)	0.7543 (3)
C6	0.7663 (3)	0.3785 (3)	0.7421 (3)
C7	0.8059 (3)	0.2993 (3)	0.6264 (2)
C8	0.9900 (3)	0.2797 (3)	0.6543 (2)
C9	1.1151 (4)	0.3496 (3)	0.6075 (3)
C10	1.2772 (4)	0.3282 (4)	0.6435 (3)
C11	1.3064 (4)	0.2407 (4)	0.7280 (3)
C12	1.1740 (4)	0.1724 (3)	0.7734 (3)
C13	1.1987 (5)	0.0781 (4)	0.8658 (4)
C14	0.6867 (5)	0.1148 (4)	0.4605 (3)
C15	0.7045 (6)	0.2623 (4)	0.4204 (3)

[a] Estimated standard deviations in the least significant digits are shown in parentheses.

Table VI. Coordinates of Non-Hydrogen Atoms for $CoCl_2C_{15}H_{16}N_2O_2$ (**7**)[a]

atom	*x*	*y*	*z*
Co	0.52274 (4)	0.30657 (3)	0.38811 (2)
Cl1	0.62895 (11)	0.30371 (8)	0.26431 (5)
Cl2	0.68133 (8)	0.37227 (7)	0.48265 (4)
O1	0.3035 (2)	0.2655 (2)	0.5119 (1)
O2	0.0717 (2)	0.1849 (2)	0.4811 (1)
N1	0.4507 (2)	0.1312 (2)	0.4016 (1)
N2	0.3125 (2)	0.3882 (2)	0.3684 (1)
C1	0.7097 (4)	0.0538 (3)	0.3764 (2)
C2	0.5401 (3)	0.0355 (3)	0.3862 (1)
C3	0.4761 (4)	−0.0792 (3)	0.3829 (2)
C4	0.3215 (4)	−0.0951 (3)	0.3931 (2)
C5	0.2304 (4)	0.0018 (3)	0.4108 (2)
C6	0.2982 (3)	0.1126 (2)	0.4167 (1)
C7	0.2126 (3)	0.2223 (2)	0.4476 (2)
C8	0.1857 (3)	0.3248 (2)	0.3887 (2)
C9	0.0393 (3)	0.3570 (3)	0.3644 (2)
C10	0.0232 (4)	0.4624 (3)	0.3212 (2)
C11	0.1495 (4)	0.5306 (3)	0.3046 (2)
C12	0.2958 (3)	0.4921 (2)	0.3282 (2)
C13	0.4368 (4)	0.5651 (3)	0.3122 (2)
C14	0.1954 (4)	0.3245 (3)	0.5640 (2)
C15	0.0498 (3)	0.2529 (3)	0.5528 (2)

[a] Estimated standard deviations in the least significant digits are shown in parentheses.

Table VII. Selected Bond Lengths (Å) and Bond Angles (deg) in Complex **10**

Ni–N1	2.124 (4)	Ni–O3	2.026 (3)
Ni–N2	2.149 (4)	Ni–O4	2.060 (4)
Ni–O1	2.113 (3)	Ni–O5	2.029 (4)
N1–Ni–N2	87.79 (15)	O3–Ni–N1	102.73 (15)
O1–Ni–O3	175.81 (15)	O3–Ni–N2	99.58 (15)
O1–Ni–O4	92.17 (18)	O4–Ni–O5	89.72 (19)
O1–Ni–O5	91.62 (15)	O4–Ni–N1	89.73 (16)
O1–Ni–N1	77.82 (14)	O4–Ni–N2	168.43 (18)
O1–Ni–N2	76.26 (14)	O5–Ni–N1	169.40 (15)
O3–Ni–O4	91.98 (17)	O5–Ni–N2	90.64 (18)
O3–Ni–O5	87.96 (17)		

Table VIII. Coordinates of Non-Hydrogen Atoms for $NiCl_2C_{15}H_{16}N_2O_2{\cdot}3H_2O$ (**10**)[a]

atom	*x*	*y*	*z*
Ni	0.56050 (3)	0.39663 (3)	0.68019 (2)
Cl1	0.66695 (6)	0.40021 (6)	0.21277 (5)
Cl2	0.17670 (6)	0.41173 (7)	0.63494 (5)
O1	0.7235 (2)	0.3710 (2)	0.65141 (8)
O2	0.8080 (1)	0.3399 (2)	0.56000 (8)
O3	0.4037 (1)	0.4291 (2)	0.70322 (9)
O4	0.5746 (3)	0.2998 (1)	0.75135 (9)
O5	0.6095 (1)	0.5049 (2)	0.73655 (9)
N1	0.5407 (1)	0.2794 (2)	0.6184 (1)
N2	0.5794 (2)	0.4895 (2)	0.6021 (1)
C1	0.3761 (2)	0.2064 (3)	0.6617 (2)
C2	0.4674 (1)	0.2065 (3)	0.6156 (1)
C3	0.4775 (3)	0.1347 (2)	0.5716 (2)
C4	0.5604 (3)	0.1335 (3)	0.5309 (2)
C5	0.6381 (2)	0.2072 (3)	0.5337 (2)
C6	0.6265 (2)	0.2776 (3)	0.5781 (1)
C7	0.7057 (2)	0.3601 (3)	0.5866 (1)
C8	0.6570 (3)	0.4533 (3)	0.5648 (2)
C9	0.6863 (3)	0.4952 (3)	0.5098 (1)
C10	0.6340 (2)	0.5792 (3)	0.4925 (2)
C11	0.5584 (2)	0.6204 (4)	0.5311 (2)
C12	0.5300 (3)	0.5724 (2)	0.5861 (1)
C13	0.4460 (2)	0.6171 (4)	0.6264 (2)
C14	0.8288 (3)	0.3299 (5)	0.6637 (1)
C15	0.8877 (1)	0.3515 (4)	0.6070 (2)

[a] Estimated standard deviations in the least significant digits are shown in parentheses.

is slightly increased [95.71 (2)°] from its ideal value. This latter effect is probably the result of the large size of the chloride ions.

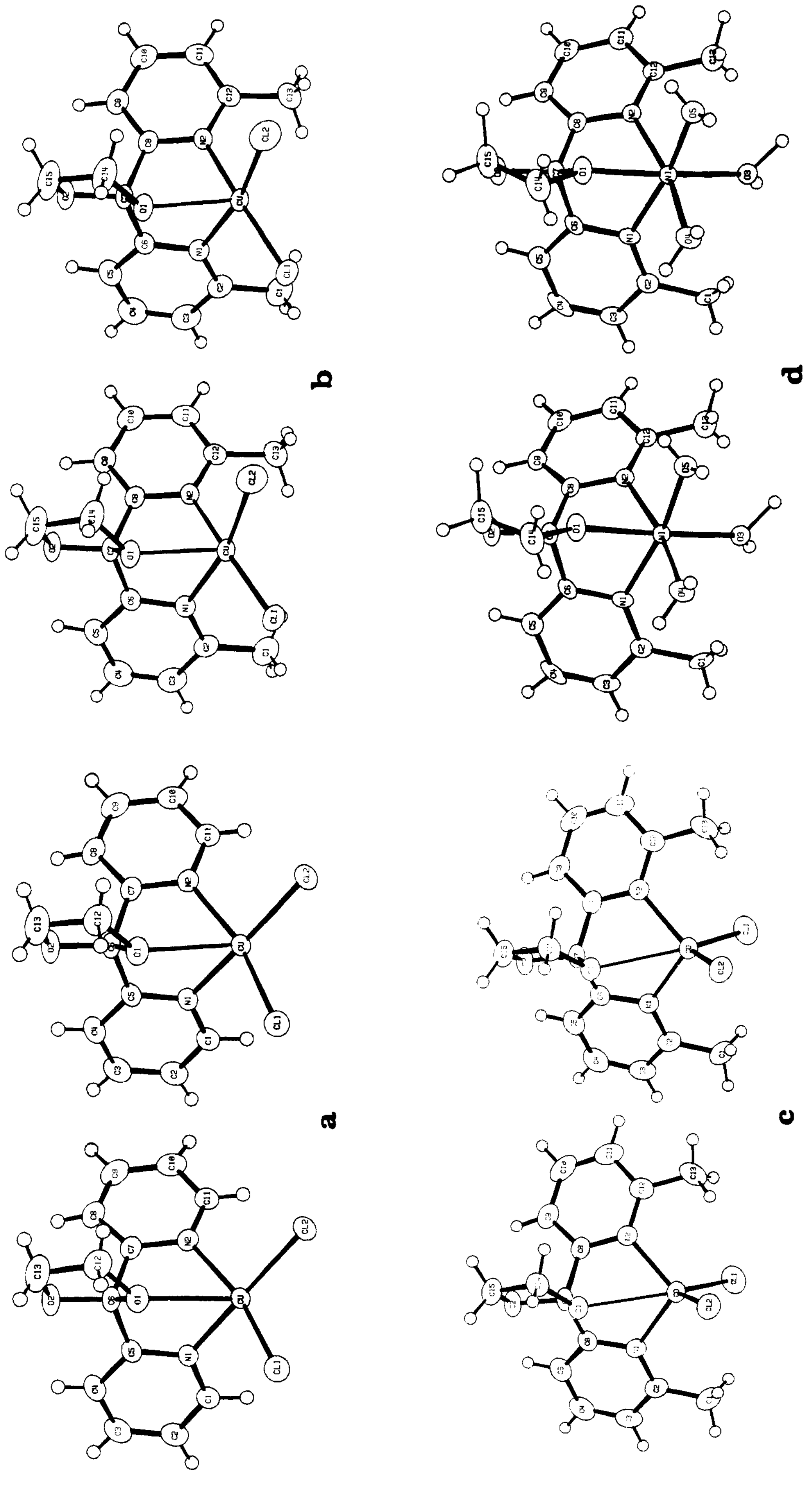

Figure 2. ORTEP stereopairs (a) **4**, (b) **5**, (c) **7**, and (d) **10**.

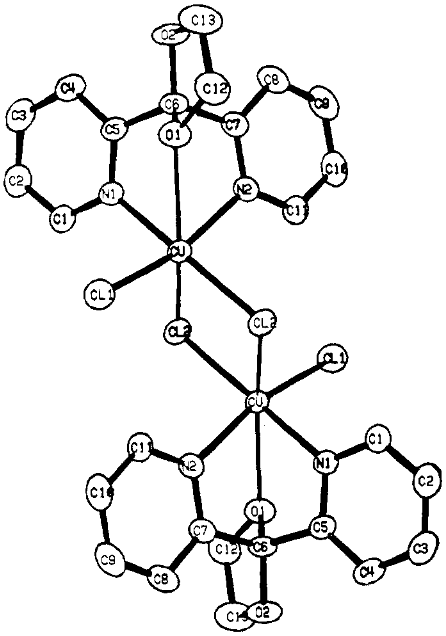

Figure 3. ORTEP of **4**. The weak interaction between two molecules results in a pseudooctahedral geometry.

The Cl–Cu–Cl plane is twisted away from the N–Cu–N plane by 17.5°; the direction of this twist is the *same* as that experienced by the dioxolane ring.

There exists another long-range interaction, between units of **4**, that serves to confer on each member of the pair a pseudooctahedral geometry. Figure 3 illustrates the tenuous linkage [intermolecular Cu–Cl2 distance of 2.844 (1) Å] supplied by the bridging chlorides. An investigation of the magnetic susceptibility of this complex as a function of temperature indicated no evidence for any Cu–Cu interaction.[14]

Dichloro[2,2-bis(6-methyl-2-pyridyl)-1,3-dioxolane]copper(II) (5). Chelation of $CuCl_2$ by **3**, under conditions similar to those above, gave a blue-green solution from which slowly crystallized massive, dark green blocks of **5**. The structure of **5** is strikingly similar to that of **4**, as the ligands differ only in the 6-substituent of the pyridine ring, which is not directly involved in chelation. Crystals of **5** are composed of neutral molecules that contain a Cu(II) held in a square-planar geometry (Figure 2b). The planar pyridines make a dihedral angle of 69.5°, but in this case the "bite" [N–Cu–N] is somewhat smaller: 81.94 (7)°. This reduction is not sufficient to alter the conformation of the chelate ring (Cu–N1–C6–C7–C8–N2); however, as above, the metal and the 2-carbon of the dioxolane (C7) lie above the plane of the other four atoms.

The conformation of the dioxolane closely approximates an envelope, in which O1 is the flap. The approach of O1 to the metal [2.400 (2) Å] is closer than in **4** but still too distant to be considered a bond. Although the reduced Cu···O1 separation would seem to imply an enhanced interaction, and thus a greater distortion of the square-planar geometry, that is not the case. The Cl1–Cu–Cl2 angle is 94.43 (3)° [as compared to 95.71 (2)° for **4**], and the dihedral angle between the Cl1–Cu–Cl2 and N1–Cu–N2 planes is only 11.6°. Furthermore, the direction of twist is *opposite* to that of the dioxolane ring. It is possible that the increased Cu–O1 interaction (diminished distance) results from a slightly more favorable position of O1 with respect to the axial site of the copper. The tilt of the Cu–O1 vector toward the pyridines is certainly lessened in **5** (Figure 2b). Thus, the direction of the axial interaction between Cu and O1 more nearly coincides with the plane normal that distortions of the plane should be reduced.

It is equally possible that these distortions are the result of more subtle effects. For one, Cu(II) is a d^9 ion and therefore susceptible to the Jahn–Teller effect.[15] Deformations, observed in the Cu(II) complexes of **2** and **3**, may serve to remove orbital degeneracy associated with the square-planar geometry and so lower the overall energy.

The only effect related to methyl substituents in **5** is in the packing within the crystal lattice; whereas two molecules of **4** formed loosely bridged dimers, such is not observed for **5**. Nonbonding interactions between a methyl group of one molecule and a chloride of the other probably disfavor an interaction of this type.

Dichloro[2,2-bis(2-pyridyl)-1,3-dioxolane]cobalt(II) (6). Treatment of **2** with $CoCl_2{\cdot}6H_2O$ in warm MeOH afforded a purple solution, from which magenta crystals of **6** were obtained upon slow evaporation. The crystals were clear and well-formed at first inspection; unfortunately, all crystals that were evaluated proved to be twinned and unsuitable for X-ray analysis.

Dichloro[2,2-bis(6-methyl-2-pyridyl)-1,3-dioxolane]cobalt(II) (7). Reaction of **3** with $CoCl_2{\cdot}6H_2O$ in warm MeOH and subsequent evaporation gave large prismatic dark blue crystals (**7**). In order to compare the behavior of **3** with different metals, an X-ray structure determination of **7** was undertaken.

Crystals of **7** consisted of neutral molecules in which the Co(II) coordination geometry is a slightly distorted tetrahedron (Figure 2c). In accordance with the previous structures, the pyridines are planar and N-chelated with a "bite" angle [99.65 (6)°] ca. 10° less than the ideal tetrahedral angle. Despite the change in geometry of Co, the chelate ring (Co–N1–C6–C7–C8–N2) maintains its familiar boat conformation, in which Co and C7 (the 2-dioxolane carbon) reside above the plane of the other four atoms.

The expected puckering of the dioxolane (C7–O1–C14–C15–O2) locates its atoms on the same side of the ligand as the metal and position O1 above the N1–Cl2–N2 face of the coordination tetrahedron. As a consequence, the Co···O1 interaction is extremely weak: the distance between these two atoms is 2.853 (2) Å, the longest observed in this series of complexes. The combination of Co–O1 interaction and the somewhat constrained N1–Co–N2 angle produced minor distortion of the tetrahedral shape: only the angle N2–Co–Cl1 [120.80 (5)°] differs appreciably from the ideal value of 109.5°. Although the Co–O1 vector tilts back toward the N1 pyridine (Figure 2c), the N1–Co–N2 plane intersects the Cl1–Co–Cl2 plane at an angle of 90.9°, very nearly the angle predicted for a tetrahedron.

Dichloro[2,2-bis(2-pyridyl)-1,3-dioxolane]nickel(II) (8). Reaction of **2** with $NiCl_2{\cdot}6H_2O$ in warm MeOH produced a dark green solution that could not be induced to crystallize. Concentration in vacuo produced **8** as a yellow powder that regenerated the green color upon dissolution in MeOH. The yellow solid is suggestive of the square-planar geometry common to many Ni(II) complexes.[15] Dissolution in a polar solvent, such as MeOH, might serve to solvate the axial positions of the metal and so change the color to the green that is associated with Ni(II) in an octahedral field. The square-planar complex should be diamagnetic and therefore amenable to ^1H NMR analysis; unfortunately, its extreme insolubility in suitable NMR solvents rendered such a study impractical.

Dichloro[2,2-bis(6-methyl-2-pyridyl)-1,3-dioxolane]nickel(II) (9). Subjection of **3** to the same conditions resulted in the formation of a dark green solution, which could be concentrated in vacuo to give **9** as a brilliant yellow powder. Slow evaporation of MeOH from **9** afforded a tiny clump of golden-yellow needles in a dark green oil. Efforts to acquire a single crystal of X-ray quality were futile. As for **8**, however, the yellow color suggested a diamagnetic square-planar complex,[15] and **9** was found to be sufficiently soluble in Me_2SO to yield a ^1H NMR spectrum. The spectrum of **9** (see Table IX) exhibited a weak but reasonably well-resolved doublet of doublets for the aromatic protons at δ 7.69, 7.48, and 7.14 for H-4, H-3, and H-5, respectively. The methylene protons resonated at δ 4.01 and those of the methyl groups at δ 2.35; both signals were singlets.

---

(14) O'Connor, C. J., unpublished results.

(15) Cotton, F. A.; Wilkinson, G. "Advanced Inorganic Chemistry", 4th ed.; Interscience: New York, 1980.

Table IX. ^1H NMR Data for Selected Transition-Metal Complexes[a]

	py					
compd (solvent)	6-H	4-H	3-H	5-H	ketal	CH_3
11 ($CDCl_3$)	9.27	7.90		7.41	4.40	...
		[4.9, 1.2]	m		[7.3, 4.9, 1.2]	m
12 ($CDCl_3$)	...	7.73		7.27	4.56	3.37
			m		[7.3, 1.2]	s
9 (Me_2SO-d_6)	...	7.69	7.48	7.14	4.01	2.35
			[7.9, 7.3]	[7.3, 1.2]	s	s

[a] Values in brackets are the coupling constants in Hz.

Triaquo[2,2-bis(6-methyl-2-pyridyl)-1,3-dioxolane]nickel(III) Chloride (10). A second attempt was made to prepare a single crystal of **9**. The yellow powder was dissolved in absolute MeOH and allowed to stand undisturbed for ca. 1 month. Evaporation of the solvent produced crystals of a habit different from that of the crystals of **9**: the light green crystals of **10** were massive and highly fractured, but one suitable for X-ray structure determination was found. Crystals of **10** consist of [Ni(**3**)·$3H_2O$] cations and Cl^- counterions; the geometry around the Ni(II) ion is almost perfectly octahedral. Selected bond distances and angles for **10** are compiled in Table VII; non-hydrogen atom coordinates are listed in Table VIII. In this complex, **3** behaves as a *tridentate ligand*,[4,6] metal chelation being achieved by virtue of the pyridine nitrogens and O1 of the dioxolane ring (Figure 2d). The N1-Ni-N2 "bite" angle is 87.79 (15)°, and the N-Ni-O1 angle is 77.82 (14)° for N1 and 76.26 (14)° for N2; the Ni-O1 bond is tilted slightly toward the heteroaromatic rings (Figure 3). The Ni-O1 distance is indicative of the relative strength of the interaction: the two atoms are separated by only 2.113 (3) Å.

Other features of this structure are much the same as observed for the related Cu(II) and Co(II) complexes. The chelate ring exists in the boat form, in which C7 (the 2-dioxolane carbon) and the metal lie above the plane of the other four atoms. The planar pyridines make a dihedral angle of 66.2°, and the dioxolane ring is puckered.

Although the solvent of crystallization was anhydrous MeOH, conversion of **9** to **10** is not difficult to understand. Nickel(II) complexes are frequently hygroscopic, and prolonged standing open to the atmosphere offered ample chance for **9** to undergo hydration.

Dichloro[2,2-bis(2-pyridyl)-1,3-dioxolane]palladium(II) (11).[12] Treatment of **2** with $PdCl_2$ in warm CH_3CN resulted in the formation of **11** as a yellow complex. The aromatic ^1H NMR spectrum of **11** (Table IX) consisted of a doublet of doublets of doublets at δ 9.27 for H-6, a multiplet at δ 7.90 that included the signals for H-3 and H-4, and a doublet of doublets at δ 7.41 for H-5. For reasons that are not yet understood, the signal for the methylenes at δ 4.40 was a symmetrical multiplet rather than the usual broad singlet. The crystal structure of **11** has recently been described.[12]

Dichloro[2,2-bis(6-methyl-2-pyridyl)-1,3-dioxolane]palladium(II) (12). Identical treatment of **3** with $PdCl_2$ also gave a yellow complex (**12**), which could not be induced to crystallize. The ^1H NMR spectrum of **12** exhibited a multiplet centered at δ 7.73 for the pyridine 3- and 4-hydrogens and a doublet at δ 7.27 for the pyridine 5-hydrogens. Singlets at δ 4.56 and 3.37 represented the ketal and methyl hydrogens, respectively. The downfield shift of the peaks is a direct consequence of coordination to the metal.

Experimental Section

A. General Comments. All melting points were taken in capillary tubes with a Thomas-Hoover Uni-Melt apparatus and are uncorrected. ^1H NMR spectra were determined on an IBM Bruker NR/80 spectrometer using $CDCl_3$, as solvent, with Me_4Si, as the internal standard. Elemental analyses were obtained commercially from Micanal Organic Microanalyses, Tucson, AZ.

B. Ligands. 2,2-Bis(2-pyridyl)-1,3-dioxolane (**2**) was prepared by a known procedure[16] while 2,2-bis(6-methyl-2-pyridyl)-1,3-dioxolane (**3**) was synthesized by condensing 2-formyl-6-methylpyridine with 2-lithio-6-methylpyridine at -90 °C, oxidizing the carbinol, and acid-catalyzed ketalizing with ethylene glycol in toluene.[17]

C. Complexes of 2 and 3 with Cu(II), Co(II), and Ni(II). General Procedures. To a solution of **2** (75 mg, 0.33 mmol) or **3** (84.5 mg 0.33 mmol) in warm MeOH (10 mL) was added a solution of the metal salt (0.30 mmol) in warm MeOH (10 mL). The mixture was refluxed overnight, open to the air. Absolute EtOH was added to azeotrope water, and the sample was concentrated in vacuo. The colored residue was washed with 1:1 EtOAc/C_6H_{12}, to remove excess ligand, and then dissolved in MeOH. Physical data are presented in Table I and IX.

Complexes of 2 and 3 with Pd(II). To a solution of **2** (75 mg, 0.33 mmol) or **3** (84.5 mg, 0.33 mmol) in warm CH_3CN (15 mL) was added a solution of $PdCl_2$ (52.5 mg, 0.30 mmol) in warm CH_3CN (30 mL). The dark orange solution was stirred overnight at 25 °C, during which time a yellow precipitate slowly formed. The solid was filtered and washed with EtOAc/C_6H_{12} (1:1) and then dissolved in $CHCl_3$. Physical data are given in Tables I and IX.

D. X-ray Experimental Procedure. Intensity data were collected by ω-2θ scans on an Enraf-Nonius CAD4 diffractometer equipped with Mo Kα radiation (λ = 0.71073 Å) and a graphite monochromator. Variable scan rates were used in order to measure all significant data with $I \approx 50\sigma(I)$. One hemisphere of data for the triclinic crystal, one quadrant for the monoclinic crystals, and one octant for the orthorhombic crystal were collected within the 2θ limits given in Table II. Data reduction included corrections for background, Lorentz, and polarization effects and absorption corrections, based upon ψ scans of reflections near χ = 90°. Crystal data and the number of unique and observed [$I > 3\sigma(I)$] data are given in Table II.

All structures were solved by the heavy-atom method and refined by full-matrix least squares, minimizing $\sum w(F_o - F_c)^2$, with weights $w = \sigma^{-2}(F_o)$, using the Enraf-Nonius SDP programs.[18] Atomic scattering factors were those of Cromer and Waber,[19] with anomalous coefficients of Cromer.[20] Non-hydrogen atoms were treated anisotropically; H atoms were located in difference maps, refined isotropically in two structures, and included as fixed contributions with B = 5.0 Å^2 in the other two (Table II). Secondary extinction effects were evident in all data sets, and extinction coefficients were refined. R factors and residual electron densities are given in Table II.

Acknowledgment. We wish to thank the National Science Foundation and LSU Center for Energy Studies for partial support of this work.

Supplementary Material Available: Tables of the bond distances, bond angles, hydrogen atom coordinates, anisotropic thermal parameters, observed and calculated structure factors, and least-squares planes for **4**, **5**, **7**, and **10** (71 pages). Ordering information is given on any current masthead page.

---

(16) Newkome, G. R.; Sauer, J. D.; McClure, G. L. *Tetrahedron Lett.* **1973**, *14*, 1599.

(17) Taylor, H. C. R. *Ph.D. Dissertation*, Louisiana State University, Baton Rouge, LA, Aug 1983; p 154.

(18) Frenz, B. A.; Okaya, Y. "Enraf-Nonius Structure Determination Package"; Enraf-Nonius: Delft, Holland, 1980.

(19) Cromer, D. T.; Waber, J. T. "International Tables for X-Ray Crystallography"; Kynoch Press: Birmingham, England, 1974; Vol. IV, Table 2.2B.

(20) Cromer, D. T. "International Tables for X-Ray Crystallography"; Kynoch Press: Birmingham, England, 1974; Vol. IV, Table 2.3.1.